PLOS ONE

RESEARCH ARTICLE

Multiplanar strain quantification for assessment of right ventricular dysfunction and non-ischemic fibrosis among patients with ischemic mitral regurgitation

Antonino Di Franco[1], Jiwon Kim[1], Sara Rodriguez-Diego[1], Omar Khalique[2], Jonathan Y. Siden[1], Samantha R. Goldburg[1], Neil K. Mehta[1], Aparna Srinivasan[1], Mark B. Ratcliffe[3], Robert A. Levine[4], Filippo Crea[5], Richard B. Devereux[1], Jonathan W. Weinsaft[1]*

1 Department of Medicine, Weill Cornell Medical College, New York City, New York, United States of America, **2** Department of Medicine, Columbia University, New York, New York, United States of America, **3** Department of Surgery, University of California San Francisco, San Francisco, California, United States of America, **4** Department of Cardiology, Massachusetts General Hospital, Boston, Massachusetts, United States of America, **5** Department of Cardiology, Università Cattolica del Sacro Cuore, Fondazione Policlinico Universitario A. Gemelli, Rome, Italy

* jww2001@med.cornell.edu

Citation: Di Franco A, Kim J, Rodriguez-Diego S, Khalique O, Siden JY, Goldburg SR, et al. (2017) Multiplanar strain quantification for assessment of right ventricular dysfunction and non-ischemic fibrosis among patients with ischemic mitral regurgitation. PLoS ONE 12(9): e0185657. https://doi.org/10.1371/journal.pone.0185657

Editor: Vincenzo Lionetti, Scuola Superiore Sant'Anna, ITALY

Received: June 12, 2017

Accepted: September 16, 2017

Published: September 29, 2017

Data Availability Statement: All relevant data are within the paper.

Funding: The work was supported by National Institutes of Health, grant # 1R01HL128278-01 (PI: Weinsaft M.D.). The funders had no role in study design, data collection and analysis, decision to publish, or preparation of the manuscript.

Competing interests: The authors have declared that no competing interests exist.

Abstract

Background

Ischemic mitral regurgitation (iMR) predisposes to right ventricular (RV) pressure and volume overload, providing a nidus for RV dysfunction (RV_{DYS}) and non-ischemic fibrosis (NIF). Echocardiography (echo) is widely used to assess iMR, but performance of different indices as markers of RV_{DYS} and NIF is unknown.

Methods

iMR patients prospectively underwent echo and cardiac magnetic resonance (CMR) within 72 hours. Echo quantified iMR, assessed conventional RV indices (TAPSE, RV-S', fractional area change [FAC]), and strain via speckle tracking in apical 4-chamber (global longitudinal strain [RV-GLS]) and parasternal long axis orientation (transverse strain). CMR volumetrically quantified RVEF, and assessed ischemic pattern myocardial infarction (MI) and septal NIF.

Results

73 iMR patients were studied; 36% had RV_{DYS} (EF<50%) on CMR among whom LVEF was lower, PA systolic pressure higher, and MI size larger (all $p<0.05$). CMR RVEF was paralleled by echo results; correlations were highest for RV-GLS ($r = 0.73$) and lowest for RV-S' ($r = 0.43$; all $p<0.001$). RV_{DYS} patients more often had CMR-evidenced NIF (54% vs. 7%; $p<0.001$). Whereas all RV indices were lower among NIF-affected patients (all $p \leq 0.006$), percent change was largest for transverse strain (48.3%). CMR RVEF was independently associated with RV-GLS (partial $r = 0.57$, $p<0.001$) and transverse strain ($r = 0.38$, $p = 0.002$) ($R = 0.78$, $p<0.001$). Overall diagnostic performance of RV-GLS and transverse

strain were similar (AUC = 0.93[0.87–0.99]|0.91[0.84–0.99], both p<0.001), and yielded near equivalent sensitivity and specificity (85%|83% and 80%|79% respectively).

Conclusion

Compared to conventional echo indices, RV strain parameters yield stronger correlation with CMR-defined RVEF and potentially constitute better markers of CMR-evidenced NIF in iMR.

Introduction

Ischemic mitral regurgitation (iMR) predisposes to right ventricular (RV) pressure and volume overload, providing a stimulus for RV dysfunction (RV_{DYS}). Echocardiography (echo) is widely used to assess iMR, but performance of different indices as markers of RV_{DYS} and tissue remodeling has not been fully elucidated. Given that RV_{DYS} impacts morbidity and mortality [1,2], validation of established and emerging echo approaches for RV assessment is of substantial importance.

Cardiac magnetic resonance (CMR) enables RV function to be volumetrically quantified, an approach that is highly reproducible and entails no geometric assumptions [3]. CMR allows assessment of myocardial tissue properties [4,5], including non-ischemic fibrosis (NIF)–a marker of response to increased RV afterload that has itself been associated with adverse prognosis [6,7]. Conventional echo RV indices have been compared to CMR in mixed cohorts, for which results have shown limited agreement with volumetric quantification via CMR [8–10].

One potential reason for discordance between CMR and echo may stem from approaches used for RV assessment. Conventional echo methods assess the RV in a single 2D orientation, which can provide limited insight into global RV performance. Recent data by our group and others have shown multiplanar echo quantification–including linear fractional shortening in apical and parasternal long axis (PLAX) views–to yield improved echo assessment of CMR evidenced RV_{DYS} [11–13]. New echo methods enable assessment of myocardial deformation (strain); utility of multiplanar strain imaging for assessment of volumetric RV_{DYS} and NIF-associated RV remodeling by CMR is unknown.

This study examined RV performance among a prospective cohort of patients with iMR undergoing echo and CMR. Goals were to (1) assess prevalence of CMR-evidenced RV_{DYS} (RV ejection fraction [EF<50%]) and septal NIF among patients with iMR; (2) compare the ability of conventional and multiplanar strain RV echo indices to act as markers of CMR-defined RV_{DYS} and NIF.

Materials and methods

Study population

Patients were enrolled prospectively from September 2015 to May 2016 as part of an established protocol examining iMR associated remodeling—approximately 20% of patients recruited agreed to enrollment. Eligible patients had documented history of MR (≥mild) and were recruited from those being considered for invasive coronary angiography at Weill Cornell Medical College, in the context of known obstructive coronary artery disease (CAD) or abnormal stress test. All patients had either obstructive CAD based on angiography or prior history of coronary revascularization/myocardial infarction (MI). Patients with primary MR (e.g. prolapse, rheumatic), papillary muscle rupture, prior mitral valve replacement, or

contraindications to CMR (NYHA IV, unstable angina, acute MI) or gadolinium (e.g. glomerular filtration rate<30 ml/min/1.73m^2) were excluded. Clinical indices (including prior MI and coronary revascularization) were attained in a standardized manner using uniform patient questionnaires (administered by research personnel at time of study imaging) and supplemented by review of medical records.

Imaging was performed at Weill Cornell Medical College (New York, NY). The Cornell Institutional Review Board approved this study (Protocol #: 1505016238R002), which was in compliance with the Declaration of Helsinki. Written informed consent was obtained at time of patient enrollment.

Imaging protocol

Echo and CMR were performed within a 3-day (72-hour) interval using a standardized protocol:

Echocardiography. Transthoracic echo was performed using commercial equipment (Philips ie33 [Andover, MA]). Echoes were interpreted by experienced investigators within a high-volume laboratory, for which expertise and reproducibility for quantitative LV and RV indices have been validated and applied in population-based research [12,14,15]. RV systolic function was quantified via TAPSE, RV-S' and fractional area change (FAC), which were acquired in accordance with consensus guidelines [16]. TAPSE was measured (on M-mode) as the systolic excursion of the lateral tricuspid annulus along its longitudinal plane. RV-S' was measured (on tissue Doppler) as the peak tricuspid annular longitudinal velocity of excursion. FAC was measured via planimetry of end-diastolic and end-systolic contours in apical 4-chamber orientation. Established cutoffs (TAPSE < 1.6 cm, S'<10 mm/s, FAC< 35%) were used to detect RV_{DYS} by each parameter [16].

Strain based indices were also quantified to further assess RV function. To test the utility of multiplanar imaging, strain was measured in two distinct orientations:

- RV longitudinal strain: Global and regional longitudinal strain were measured in 2D apical 4 chamber datasets, for which images were acquired at frame rates of 60–90 Hz. Endocardial tracking points (from tricuspid annulus through RV apex) were placed at end-systole; automated tracking was used to propagate seed points throughout the cardiac cycle and, when required, were manually adjusted by an experienced reader (ADF) to ensure optimal border tracking and deformation curves. Global longitudinal strain (GLS) was calculated as mean of all RV seed points; regional strain was assessed in the inferoseptum and inferior RV free wall (each of which were analyzed as discrete segments).
- RV transverse strain was measured in 2D PLAX. Seed points were placed throughout the superior RV free wall and anteroseptum, encompassing the RV chamber as visualized in PLAX (Fig 1A): Systolic excursions of the RV free wall (in relation to the septum) was measured as "transverse strain" (Fig 1B), which was calculated as a singular discrete variable reflecting the mean of all seed point excursions in the RV superior free wall and anteroseptum.

RV-GLS and transverse strain were assessed in relation to one another as singular indices, each of which reflected global RV excursions in respective orientations (apical 4 chamber, PLAX).

Intra- and inter-observer reproducibility assessments of strain indices (RV-GLS, transverse strain) were determined via blinded repeat analyses of 20 patients. Strain analyses were

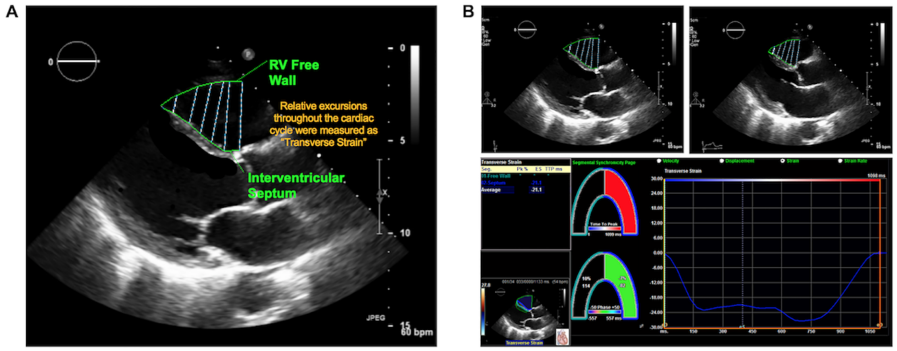

Fig 1. Illustration of analytic method for quantification of transverse strain. 1A. PLAX images were analyzed via placement of contour lines in the RV free wall and anteroseptum; transverse strain was calculated as relative excursions of the RV free wall in relation to the septum. **1B**. Data output generated from PLAX transverse strain segmentation method. Primary images (end-diastole [left], end-systole [right]) with superimposed strain contours shown on top; resultant strain output and curve shown on bottom.

https://doi.org/10.1371/journal.pone.0185657.g001

performed using commercial software (TomTEC [Munich, Germany]) and are reported as absolute values.

Additional analyses were performed to assess ancillary echo indices relevant to RV remodeling. MR severity was measured quantitatively in all patients using regurgitant fraction and/or vena contracta. To account for differences in individual indices, MR severity was also graded in accordance with consensus guidelines [17] using a 5-point (0–4+) scale based on aggregate data yielded by vena contracta, volumetric indices, jet depth as well as mitral and pulmonary vein flow pattern [18,19]. LV systolic function, geometry, and mass were quantified based on linear dimensions in parasternal long axis, consistent with quantitative methods previously validated in necropsy-comparison and population-based outcomes studies [20–23].

Cardiac magnetic resonance. CMR was performed using 3.0 Tesla scanners (General Electric, Waukesha, WI). Exams consisted of two components: (1) cine-CMR for geometry/function and (2) delayed enhancement (DE-) CMR for tissue characterization. Cine-CMR was performed using a steady-state free precession sequence. DE-CMR was performed 10–30 minutes after administration of gadolinium (0.2 mmol/kg) using a segmented inversion recovery sequence, with inversion time tailored to null viable myocardium. Cine- and DE-CMR were obtained in matching LV short and long-axis planes. LV infarct size was measured on DE-CMR, for which transmural extent and regionality was scored using a 17-segment model: Infarct size was graded based on transmural extent of hyperenhancement; global infarct size (% LV myocardium) was calculated by summing all segmental scores (weighted by the midpoint of hyperenhancement range) and dividing by total number of regions [24,25].

DE-CMR was also used to identify NIF, which was defined as localized hyperenhancement in the mid myocardial or epicardial aspect of the basal to mid inter-ventricular septum (Fig 2), in accordance with prior research by our group and others [26–28]. Cine-CMR was used to assess RV and LV geometry/function: End-diastolic and end-systolic chamber volumes were measured in contiguous short axis images, with results used to calculate EF. Cine-CMR quantified RVEF was employed as the reference standard for RV_{DYS}, which was defined using an established binary cutoff (RVEF$<$ 50%) [11,29–31]. CMR analyses were performed by an experienced reader (JWW), for whom high reproducibility for both LV and RV indices has been documented [12,32,33].

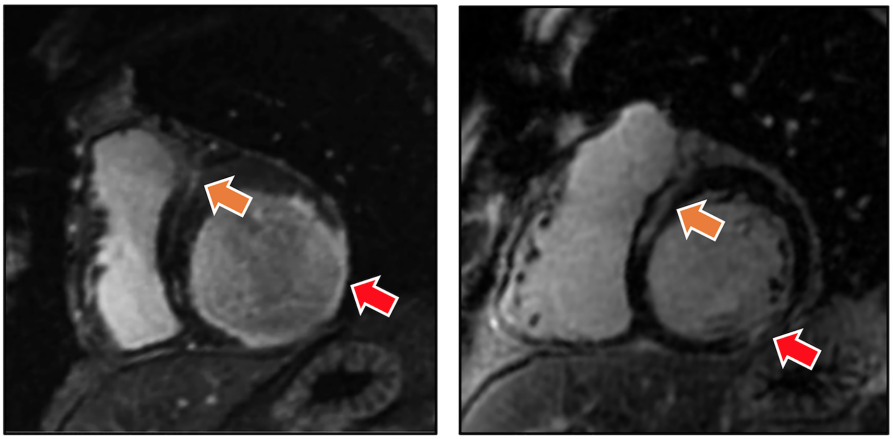

Fig 2. Representative examples of ischemic (red arrows) and non-ischemic (orange arrows) patterns of late gadolinium enhancement demonstrated by DE-CMR among patients with iMR and RV_{DYS}. Note concomitant NIF (localized to the mid-myocardial aspect of the interventricular septum) and CAD pattern transmural MI.

https://doi.org/10.1371/journal.pone.0185657.g002

Statistical analysis

Continuous variables (expressed as mean±standard deviation) were compared using Student's t-tests. Categorical variables were compared using Chi-square or, when fewer than 5 expected outcomes per cell, Fisher's exact test. Ordinal comparisons (i.e. MR grade) were performed using the Mann-Whitney U test. Correlation coefficients, as well as univariable and multivariable regression analyses were used to evaluate associations between continuous variables. Inter-observer and intra-observer agreement between methods was assessed using Bland and Altman analysis, including mean difference and limits of agreement between measurements (mean±1.96 SD). Percent changes were calculated by means of the following formula (with the larger mean always used in the denominator):

$$\frac{(\text{mean value Group 1}) - (\text{mean value Group 2})}{(\text{mean value Group 1})} * 100$$

Cohen's D test was used to measure "effect size". Two- sided $p<0.05$ was considered indicative of statistical significance. Statistical calculations were performed using SPSS 20.0 (SPSS Inc, Chicago, IL).

Results

Population characteristics

The population comprised 73 patients with iMR who underwent CMR and echo within mean interval of 0.2±0.6 days (96% same day). Over one third (36%) of patients had RV_{DYS} (EF<50%) as defined by the reference standard of CMR: Among affected patients, RV_{DYS} magnitude varied (RVEF<30%: 19% [n = 5] | 30–40%: 23% [n = 6] | 41–49%: 58% [n = 15]). Obstructive CAD was confirmed via invasive angiography in 95% (69/73) of patients (84% multivessel CAD)–all remaining patients had a history of prior PCI and/or ECG/imaging localized inferolateral MI. Clinically reported MI was present in nearly 2/3 (64%) of patients (mean interval 2.6±4.2 years prior to CMR). MI incidence as identified by DE-CMR (i.e. CAD pattern infarction) was slightly higher (83%) than that of clinical MI: Nearly a third of patients

in the overall cohort (29%) had multiple DE-CMR evidenced infarcts in distinct coronary arterial territories.

Table 1 details clinical and imaging characteristics of the population, as well as comparisons between patients with and without RV_{DYS}. As shown, patients with RV_{DYS} were similar with respect to CAD risk factors, but were more likely to require heart failure medications such as ACE inhibitors or loop diuretics, consistent with larger MI size and higher pulmonary artery (PA) pressure (all $p<0.05$). Both CMR and echo demonstrated patients with RV_{DYS} to have more advanced adverse LV remodeling, whether measured by LVEF or LV chamber size (both $p<0.05$). Consistent with this, MR severity was strongly linked to RV contractile impairment, as evidenced by nearly a 2.5-fold increase in prevalence of advanced (≥moderate) MR among patients with, compared to those without, RV_{DYS} (73% vs. 30%, $p = 0.001$). In multivariate analysis, RV_{DYS} was independently associated with advanced MR (OR 6.1 [95% CI 1.7–21.4]; $p = 0.005$) even after controlling for magnitude of CMR-defined LV dysfunction (OR 2.0 per 10-point decrement in LVEF [CI 1.4–2.6] $p< 0.001$) (model $\chi^2 = 32.95$, $p<0.001$) (Table 2). Substitution of echo derived LVEF in the model yielded similar results, again showing RV_{DYS} to be associated with advanced MR (OR 5.5 [95% CI 1.6–19.3]; $p = 0.008$) independent of global LV dysfunction (OR 2.0 per 10-point decrement in LVEF [95% CI 1.5–2.6]; $p< 0.001$) (model $\chi^2 = 32.98$, $p< 0.001$).

Apical echocardiographic indices of RV function

RV volumetric measurements were compared to echo strain and conventional indices of RV performance as measured in apical 4-chamber orientation: Nearly all exams (93%) yielded full datasets inclusive of TAPSE, RV-S', FAC, and RV-GLS. RV-GLS, in particular, was obtained in 97% (71/73) of exams.

Table 3 reports echo-derived variables, including comparisons between patients with and without CMR defined RV_{DYS}. As shown, whereas all echo variables differed significantly between groups (all $p\leq0.001$), percent changes were larger for longitudinal strain compared to conventional indices. For example, RV-GLS was 1.6-fold lower among patients with RV_{DYS}, whereas TAPSE, RV-S' and FAC yielded differences of 1.3–1.4 fold. Consistent with this, data shown in Fig 3 demonstrate that correlations between CMR RVEF and echo RV-GLS ($r = 0.73$) were higher than those yielded by TAPSE ($r = 0.46$), RV-S' ($r = 0.43$) or FAC ($r = 0.61$) (all $p<0.001$).

CMR tissue characterization in relation to echo-based RV assessment

Despite angiographic-evidenced CAD, tissue characterization via CMR demonstrated septal NIF to be common in patients with iMR: NIF was present in 24% of the population, and was 8-fold more common in patients with RV_{DYS} (54% vs. 7%; $p<0.001$). Patients with NIF had more advanced RV_{DYS} and adverse remodeling on cine-CMR, as evidenced by lower RVEF (41.4±9.6 vs. 54.6±10.7%, $p< 0.001$), larger chamber size (RV end diastolic volume: 177.2±61.8 vs. 144.4±45.2 ml, $p = 0.02$), and higher PA pressure (51.7±21.9 vs. 33.6±10.7 mmHg, $p<0.001$). Regarding distribution, NIF most commonly localized to the anteroseptum (anteroseptum only: 59%|inferoseptum only: 12%|anterior and inferoseptum: 29%).

Given that NIF commonly localized to the anteroseptum (not encompassed via 4 chamber orientation), strain analysis was also performed in PLAX (an orientation that enables assessment of anteroseptal transverse displacement). PLAX derived RV transverse strain was obtainable in 92% (67/73) of exams.

Reproducibility was good for both RV-GLS and transverse strain, with small mean differences (intra-observer: 0.08±2.49 vs. 1.9±5.08, respectively; inter-observer: -1.81±3.64 vs. 0.9

Table 1. Clinical and imaging characteristics.

	Overall (n = 73)	RV_{DYS} – (n = 47)	RV_{DYS} + (n = 26)	p
CLINICAL				
Age (years)	68.3±9.9	68±9	70±11	0.38
Male gender	61 (84%)	37 (79%)	24 (92%)	0.19
Body Surface Area	1.9±0.2	1.9±0.3	1.9±0.2	0.63
Coronary Artery Disease Risk Factors				
Hypertension	58 (80%)	39 (83%)	19 (73%)	0.32
Hypercholesterolemia	55 (75%)	37 (79%)	18 (69%)	0.37
Diabetes Mellitus	39 (53%)	24 (51%)	15 (58%)	0.59
Tobacco Use	43 (59%)	26 (55%)	17 (65%)	0.40
Family History	17 (23%)	11 (23%)	6 (23%)	0.98
Prior Coronary Revascularization (PCI or CABG)	58 (80%)	36 (77%)	22 (85%)	0.42
Prior CABG	26 (36%)	15 (32%)	11 (42%)	0.38
Prior Myocardial Infarction*	47 (64%)	29 (62%)	18 (69%)	0.61
Clinical Symptoms				
Angina	44 (60%)	26 (55%)	18 (69%)	0.25
Dyspnea	58 (80%)	36 (77%)	22 (85%)	0.42
Cardiovascular Medications				
Beta-blocker	60 (82%)	38 (81%)	22 (85%)	0.76
ACE-Inhibitor or ARB	42 (58%)	22 (47%)	20 (77%)	**0.013**
Loop diuretic	26 (36%)	11 (23%)	15 (58%)	**0.003**
Statins	59 (81%)	38 (81%)	21 (81%)	0.99
Aspirin	62 (85%)	41 (87%)	21 (81%)	0.51
Thienopyridine	32 (44%)	20 (43%)	12 (46%)	0.81
CARDIAC MAGNETIC RESONANCE				
Left Atrial / Mitral Apparatus Remodeling				
Left atrial area (cm^2)	27.7±7.0	26.3±7.0	30.4±6.2	**0.014**
Left atrial diameter (cm)	4.3±0.7	4.1±0.5	4.6±0.7	**0.001**
Mitral valve tenting area– 4 chamber (cm^2)	1.8±0.9	1.6±0.9	2.0±0.8	**0.037**
Left Ventricle				
Ejection fraction (%)	42.4±16.0	48.7±14.4	31.1±12.2	**<0.001**
Stroke volume (ml)	79.4±24.7	85.0±24.5	69.2±22.2	**0.008**
End-diastolic volume (ml)	202.7±61.9	186.3±60.1	232.4±54.6	**0.002**
End-systolic volume (ml)	123.4±63.4	101.3±56.7	163.3±55.5	**<0.001**
Myocardial mass (g)	160.0±44.3	153.1±48.4	172.7±32.7	0.07
Sphericity index	0.5±0.1	0.45±0.09	0.54±0.09	**<0.001**
Myocardial Infarction˚	60 (83%)	36 (78%)	24(92%)	0.19
Global MI Size (% LV myocardium)	9.8±9.2	8.0±8.9	13.1±9.0	**0.02**
Anterior MI (% myocardium)	1.7±2.9	1.6±3.1	1.8±2.6	0.74
Lateral MI (% myocardium)	3.5±5.4	3.0±5.3	4.6±5.7	0.22
Inferior MI (% myocardium)	3.1±4.6	2.4±4.1	4.4±5.1	0.08
Multiple Myocardial Infarctions	21 (29%)	11 (24%)	10 (39%)	0.19
Right Ventricle				
Ejection fraction (%)	51.7±11.9	58.8±6.6	38.9±7.9	**<0.001**
Stroke volume (ml)	74.8±20.8	79.9±21.9	65.6±14.9	**0.002**
End-diastolic volume (ml)	151.5±51.1	138.7±43.0	174.7±56.9	**0.003**
End-systolic volume (ml)	76.5±42.6	58.4±23.7	109.1±49.7	**<0.001**

(*Continued*)

Table 1. (*Continued*)

	Overall (n = 73)	RV_{DYS} − (n = 47)	RV_{DYS} + (n = 26)	p
ECHOCARDIODIOGRAPHY				
Mitral Regurgitation				
Regurgitant Fraction (%)	39.2±14.6	35.9±14.8	43.9±13.3	**0.03**
Vena Contracta	0.3±0.1	0.3±0.1	0.4±0.1	**0.02**
Mitral regurgitation severity (grade 1–4)	40(55%) | 22 (30%) 7(10%) | 4(6%)	33 (70%) | 10(21%) 3(6%) | 1(2%)	7(27%) | 12(46%) 4(15%) | 3(12%)	**<0.001**
Advanced mitral regurgitation (≥moderate)	33 (45%)	14 (30%)	19 (73%)	**0.001**
Left Ventricle				
Ejection fraction (%)	41.9±15.9	48.1±14.8	30.6±10.8	**<0.001**
End-diastolic diameter (cm)	5.9±0.6	5.7±0.6	6.2±0.6	**0.004**
End-systolic diameter (cm)	4.7±0.9	4.4±0.8	5.3±0.7	**<0.001**
Myocardial mass (g)	212.9±69.2	207.8±74.6	222.2±58.5	0.40
Pulmonary Arterial Pressure[§] (mmHg)	38.0±16.1	34.3±14.5	44.4±16.9	**0.02**
Pulmonary Hypertension[§]	30 (41%)	15 (32%)	15 (58%)	**0.032**

Data (continuous indices) presented as mean ±standard deviation.

*Myocardial infarction classified based on clinical history/prior medical records

˚Assessed in 99% of population (n = 1; gadolinium not administered due to IV malfunction)

[§]Available in 78% of population (pulmonary hypertension defined as PA systolic pressure > 35mmHg)

https://doi.org/10.1371/journal.pone.0185657.t001

±6.25, respectively) although limits of agreement were wider for transverse strain than for RV-GLS (intra-observer: -8.0 to 11.9 vs. -4.8 to 4.9, respectively; inter-observer: -11.4 to 13.1 vs. -8.9 to 5.3, respectively) (Fig 4).

As shown in Fig 5A, PLAX transverse strain was lower among iMR patients with, vs. those without, CMR-defined RV_{DYS} (13.2±6.6 vs. 26.2±6.2%, $p< 0.001$)–magnitude of difference in terms of "effect size" was equivalent to that yielded by RV-GLS (2.0 vs 2.1, respectively). Consistent with this, data shown in Fig 5B demonstrate that transverse strain correlated with CMR

Table 2. RV_{DYS} in relation to MR and LV_{DYS}.

	Univariate Regression		Multivariate Logistic Regression *Model* $\chi^2 = 32.95$, $p<0.001$	
	Odds Ratio (95% Confidence Interval)	P	Odds Ratio (95% Confidence Interval)	P
Advanced MR (≥moderate)	6.4 (2.2–18.6)	**0.001**	6.1 (CI 1.7–21.4)	**0.005**
LVEF (per 10% decrement)	2.0 (1.5–2.6)	**<0.001**	2.0 (CI 1.4–2.6)	**<0.001**

https://doi.org/10.1371/journal.pone.0185657.t002

Table 3. Conventional echo RV functional indices.

	Overall (n = 73)	RV_{DYS} − (n = 47)	RV_{DYS} + (n = 26)	P	%Δ	Effect Size
TAPSE (cm)	1.8±0.4	1.9±0.4	1.5±0.3	**<0.001**	**21.1**	**1.1**
RV-S' (cm/sec)	11.0±2.9	12.0±2.8	9.3±2.3	**<0.001**	**22.5**	**1.1**
FAC (%)	38.2±8.8	42.2±6.1	31.1±8.4	**<0.001**	**26.3**	**1.5**
RV global longitudinal strain (%)	18.3±5.3	21.2±3.4	13.3±4.2	**<0.001**	**37.3**	**2.1**
RV free wall longitudinal strain (%)	18.1±6.6	21.5±4.3	12.3±5.8	**<0.001**	**42.8**	**1.8**
RV septal longitudinal strain (%)	11.1±6.8	13.2±6.5	7.6±5.9	**0.001**	**42.4**	**0.9**

https://doi.org/10.1371/journal.pone.0185657.t003

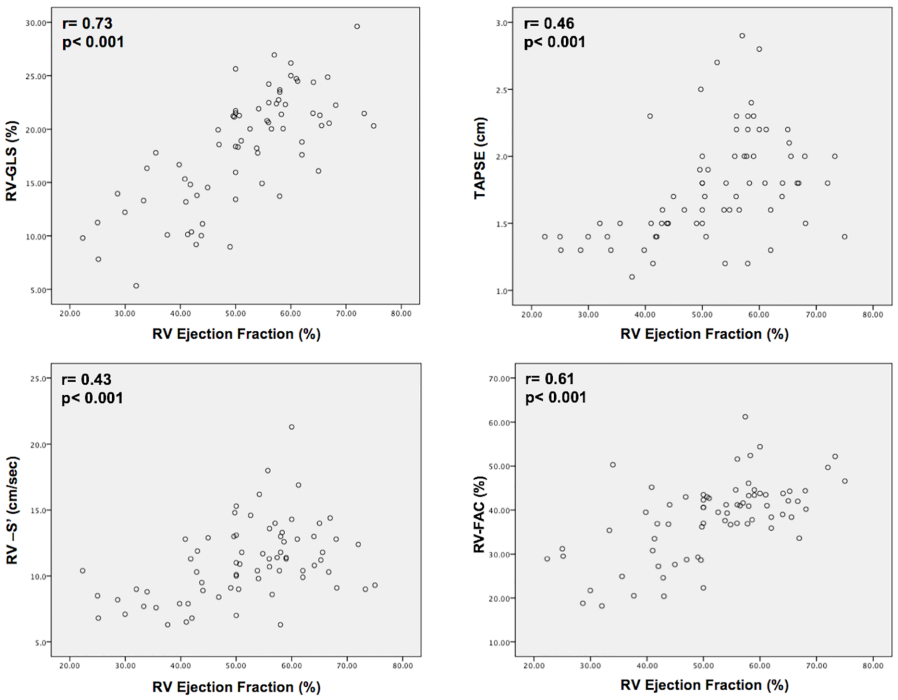

Fig 3. Scatter plots comparing conventional echo RV parameters in relation to CMR RVEF. Whereas all echo indices correlated with volumetric RVEF (p<0.001), RV-GLS (upper left) yielded higher correlations than did TAPSE, RV-S' or FAC.

https://doi.org/10.1371/journal.pone.0185657.g003

RVEF (r = 0.65; p< 0.001). RV-GLS and PLAX transverse strain yielded similar overall performance for diagnostic assessment of NIF as identified by DE-CMR (AUC: 0.87 [GLS], 0.88 [transverse]; both p<0.001). Of note, whereas all echo RV indices differed significantly between patients with and without NIF (all p<0.01), percent change was larger for transverse strain as compared to RV-GLS or conventional indices (Fig 5C) (Table 4). In multivariate

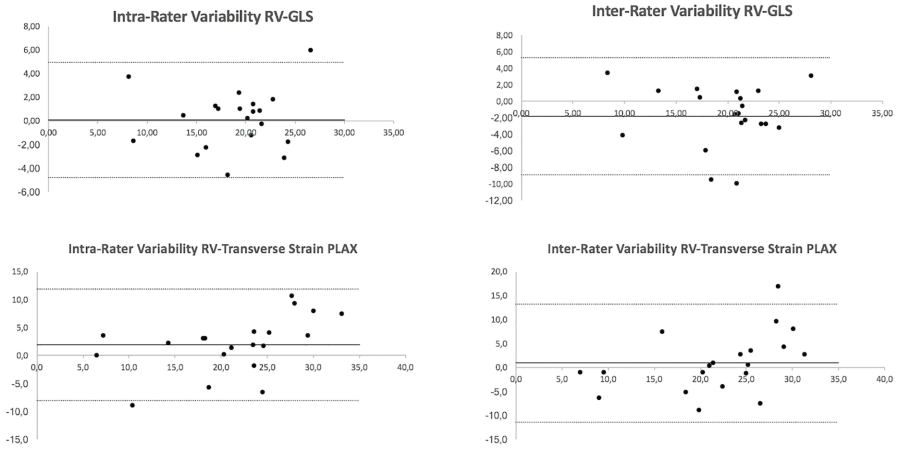

Fig 4. Bland-Altman plots demonstrating magnitude of intra- and inter-observer agreement for RV-GLS (top) and transverse strain (bottom).

https://doi.org/10.1371/journal.pone.0185657.g004

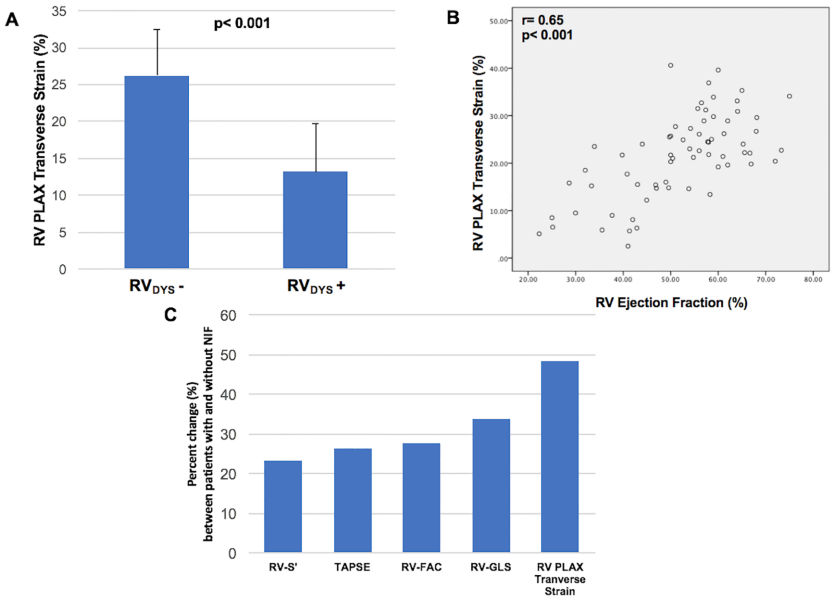

Fig 5. 5A. PLAX transverse strain values among patients with and without CMR-defined RV_{DYS} (EF<50%). Data reported as mean ± standard deviation. **5B**. Correlation between transverse strain and CMR-RVEF. **5C**. Percent change (%) between patients with and without NIF as yielded by respective echo RV parameters. Note larger percent change for transverse strain compared to other echo indices.

https://doi.org/10.1371/journal.pone.0185657.g005

analysis, RVEF on CMR was independently associated with both echo-quantified RV-GLS (partial correlation coefficient [r] = 0.57, p<0.001) as well as transverse strain (r = 0.38, p = 0.002) (model R = 0.78, p<0.001) (Table 5).

Diagnostic performance of echo indices for CMR defined RV dysfunction

Fig 6 provides superimposed ROC analyses for RV-GLS and transverse strain. As shown, overall diagnostic performance for each parameter was of similarly high magnitude (AUC 0.93 [0.87–0.99], p<0.001 and 0.91 [0.84–0.99], p<0.001, respectively). Using a matched specificity cutoff of 80%, RV-GLS yielded a sensitivity of 85% (cut-off value for RV-GLS: 18%). Similarly, transverse strain yielded a sensitivity of 83% (cut-off value for transverse strain: 21%).

Table 4. Echo strain indices stratified between patients with and without CMR-evidenced NIF*.

	NIF − (n = 55)	NIF + (n = 17)	P	%Δ	Effect Size
TAPSE (cm)	1.9±0.4	1.4±0.1	**<0.001**	26.3	1.7
RV-S' (cm/sec)	11.6±2.9	8.9±1.8	**0.001**	23.3	1.1
FAC (%)	40.9±7.5	29.5±7.2	**<0.001**	27.9	1.6
RV global longitudinal strain (%)	20.0±4.6	13.2±3.9	**<0.001**	34.0	1.6
RV free wall longitudinal strain (%)	20.2±5.8	11.6±5.1	**<0.001**	42.6	1.6
RV septal longitudinal strain (%)	12.3±6.7	7.3±6.0	**0.006**	40.7	0.8
RV transverse strain (%)	24.0±7.6	12.4±6.4	**<0.001**	48.3	1.7

* Assessed in 99% of population (n = 1; gadolinium not administered due to IV malfunction)

https://doi.org/10.1371/journal.pone.0185657.t004

Table 5. CMR RVEF in relation to echo global longitudinal and transverse strain.

	Univariate Correlations		Multivariate Linear Regression *Model R = 0.78, p<0.001*	
	Correlation Coefficients	**P**	**Partial Correlation**	**P**
Global Longitudinal Strain	0.73	**<0.001**	0.57	**<0.001**
Transverse Strain	0.65	**<0.001**	0.38	**0.002**

https://doi.org/10.1371/journal.pone.0185657.t005

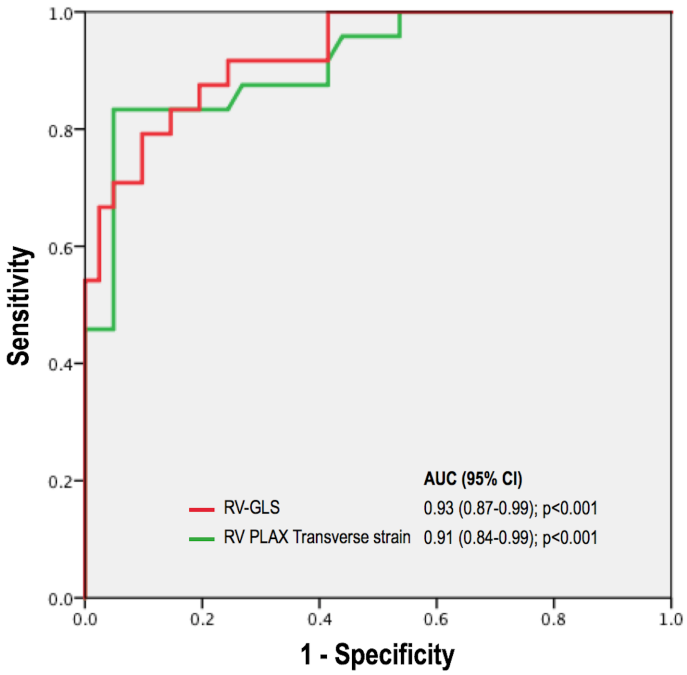

Fig 6. Superimposed receiver operating curve (ROC) analyses for RV-GLS and transverse strain, demonstrating high overall diagnostic performance (AUC > 0.90) for both strain indices.

https://doi.org/10.1371/journal.pone.0185657.g006

Diagnostic performance parameters of strain and conventional indices are reported in Table 6. As shown, transverse strain yielded good overall accuracy (81%), which was similar to RV-GLS and conventional echo parameters as acquired in apical 4-chamber orientation (76–85%).

Table 6. Diagnostic test performance of both apical and PLAX echo indices of RV function.

	Sensitivity	Specificity	PPV	NPV	Accuracy
TAPSE*	76%	85%	73%	87%	82%
RV-S'*	71%	81%	65%	83%	76%
FAC*	65%	96%	89%	83%	85%
RV global longitudinal strain**	85%	80%	71%	90%	82%
RV PLAX transverse strain**	83%	79%	69%	89%	81%

* Tested using cutoffs included in consensus guidelines (TAPSE <1.6 cm; RV-S'<10 cm/sec; FAC<35%) [16]

**Tested using cutoffs (RV-GLS 18%, transverse strain 21%) derived from ROC analysis (Fig 6).

https://doi.org/10.1371/journal.pone.0185657.t006

Discussion

This study yields new insights regarding RV pathophysiology in patients with iMR, as well as novel echo methods for assessment of RV_{DYS}. Major findings are as follows: (1) Among a cohort of patients with iMR, RV_{DYS} was common and strongly associated with LV dilation and contractile dysfunction (all $p<0.05$) measured by both CMR and echo. (2) Conventional and longitudinal strain indices differed between patients with and without CMR-evidenced RV_{DYS}, but RV-GLS yielded higher correlations with RVEF (r = 0.73) than did FAC, TAPSE, and RV-S' (r = 0.43–0.61; all $p<0.001$). Transverse strain yielded similar correlation with CMR RVEF (r = 0.65; $p<0.001$) as did RV-GLS, as well as similar overall diagnostic performance for RV_{DYS} (EF<50%) (AUC 0.91 [0.84–0.99], 0.93 [0.87–0.99] respectively [both $p<0.001$]). (3) Despite epicardial CAD, patients with iMR commonly had CMR-evidenced NIF (24%), which was 8-fold more prevalent among those with RV_{DYS} (54% vs. 7%; $p<0.001$). NIF was associated with lower RV-GLS (measured in 4-chamber orientation) and transverse strain (measured in PLAX) (both $p<0.001$). Percent change between patients with and without NIF was highest for RV transverse strain (48.3%) compared to RV-GLS (34.0%), TAPSE (26.3%), RV-S' (23.3%), and FAC (27.9%).

Our finding of an association between volumetric RVEF and transverse strain–a measure of RV free wall contractility–builds upon a growing body of literature concerning utility of multiplanar echo for RV assessment. 3D echo has been shown to improve RV quantification compared to conventional echo approaches derived from data acquired in a single orientation, and yield improved agreement with CMR [34–36]. Utility of quantitative RV assessment in multiple orientations has also been shown using 2D echo. Among 272 CAD patients undergoing CMR and echo, our group showed echo linear RV dimensions in multiple orientations to increase in proportion to CMR-evidenced RV chamber volumes [12]. This concept was subsequently tested among patients with and without biventricular heart failure, in whom CMR-quantified RVEF was independently associated with linear fractional shortening in PLAX (partial correlation r = 0.50, $p<0.001$) and apical 4 chamber orientation (r = 0.40, $p<0.001$) [11]. Our current study extends on this using strain–a newly available quantitative method that assesses aggregate contractility in a given plane rather than in an isolated linear dimension. Paralleling findings of our prior studies, RVEF was independently associated with both transverse (partial correlation r = 0.38, p = 0.002) and global strain (r = 0.57, $p<0.001$; model $R = 0.78$, $p<0.001$). These data support the concept that RV_{DYS} reflects a global process in patients with iMR (due to regurgitation-associated increments in RV afterload) that can be well assessed via multiplanar imaging.

Magnitude of correlation between strain indices and RVEF in our cohort is consistent with that reported in prior studies. However, prior studies have varied with respect to interval between testing, and no prior study has focused on RV strain in the context of MR. Among 135 post-MI patients, Lemarie et al. reported that RV-GLS yielded a higher correlation with CMR RVEF (r = 0.46) than did TAPSE (r = 0.26), RV-S' (r = 0.18), or FAC (r = 0.37). [37] Prior reports on patients with advanced LV_{DYS} have demonstrated stronger correlations between echo strain and CMR. For example, among 57 patients with ischemic cardiomyopathy (LVEF<40%), Park et al. reported that RV-GLS correlated well with CMR RVEF (r = 0.80) [38], consistent with our findings (r = 0.73). In our study, improved correlations with CMR RVEF yielded by strain were not accompanied by marked increments in diagnostic performance for RV_{DYS} using a binary threshold of RVEF <50%. For example, RV-GLS yielded sensitivity and specificity of 85% and 80% respectively, whereas respective values for TAPSE were 76% and 85%. We speculate that whereas strain provides incremental utility as a continuous index of RVEF (accounting for improved correlation coefficients), conventional indices

provide a reasonable binary means of discriminating between patients with and without RV_{DYS}. It is also important to note that all echoes in our study were specifically performed for research purposes, and were thus of higher quality than might be anticipated in general clinical practice.

Beyond RV function, it is important to note that whereas our cohort consisted of iMR patients with epicardial CAD, 24% of all patients (including 54% of those with RV_{DYS}) had NIF identified by CMR tissue characterization. To the best of our knowledge, this is the first study to assess the impact of NIF on RV_{DYS} in the setting of patients with iMR as well as its relationship with RV strain. Our finding of an association between NIF and iMR is consistent with prior basic science studies showing MR to induce up-regulation of pro-inflammatory cell-signaling pathways promoting adverse remodeling [39,40]. Up-regulation of pro-fibrotic signaling pathways has also been suggested as a potential contributing factor in the pathophysiology of NIF. In a rat model of hypoxia-induced pulmonary hypertension, McKenzie et al. reported that expression of atrial natriuretic peptide—a vasodilatory peptide secreted in pathologic conditions of increased myocardial load—was most prominent in the RV insertion points and the interventricular septum (corresponding to NIF location on CMR) [41]. Evidence that NIF might contribute to ventricular failure (rather than being a sequela) has recently been suggested in patients with LV_{DYS}. Among patients with non-ischemic cardiomyopathy, Taylor et al. demonstrated NIF to be associated with decreased global LV circumferential strain ($p = 0.004$) as measured via feature tracking CMR [42]. Our results indicate that NIF is similarly paralleled by RV strain impairments as measured via echo speckle tracking.

Regarding mechanistic links between NIF, RV_{DYS} and iMR, it should be noted that prior studies have shown NIF to be associated with RV_{DYS} and adverse RV remodeling–including work by our group which has linked NIF to increased RV wall stress [26]. These data suggest a mechanism whereby iMR results in increased PA pressure, which produces afterload-associated decrements in RV contractile function as well as NIF. It is also known that iMR can result from (and contribute to) LV chamber dilation–a known cause of increased LV wall stress that has itself been associated with NIF [28]. Increased septal stiffness as can result from NIF would be expected to further impede RV mechanics, resulting in further decrements in RV contractility as manifest via both decreased RVEF and impaired strain. Taken together with prior literature, our data suggest that NIF may be both a consequence of and contributor to adverse remodeling irrespective of ventricular chamber involvement.

Several limitations should be noted. First, this study assessed RV physiology in patients with iMR and thus it is uncertain whether results can be extrapolated to other etiologies of MR. On the other hand, a primary sequela of MR (irrespective of etiology) is right-sided pressure and volume overload–known stimuli for RV_{DYS} as well as NIF. Second, transverse strain was measured in PLAX rather than a tailored RV orientation, and regional RV strain in PLAX was not quantified as has been the case for apical 4-chamber derived RV strain. Nevertheless, to the best of our knowledge, this is the first study to assess RV deformation in an orientation different than apical 4-chamber. PLAX, in particular, is a well-established standardized orientation encompassed in nearly all echo exams, and allows for RV evaluation in a plane other than apical 4 chamber (which assesses the inferior RV). Given that apical 4 chamber derived measurements are increasingly being applied for analysis of segmental RV strain [43], future research is needed to test utility of regional strain assessment as quantified in PLAX. Third, it should be noted that our study tested utility of multiplanar imaging using conventional 2D data, rather than 3D echo. Despite this, whereas 3D echo has been shown to yield improved RV assessment [34–36], its widespread use remains limited due to both commercial factors as well as technical challenges, emphasizing the continued importance of 2D echo approaches for both clinical purposes and population-based research. It is also important to note that all

echoes in our study were performed for research purposes, and were thus of higher quality than might be anticipated in general clinical practice such that study results reflect a potential "best case scenario" with respect to performance of both transverse and longitudinal strain. It should also be noted that our study included patients who had undergone CABG. Given that prior literature has suggested that cardiac surgery itself can transiently impact RV function [44,45], it is possible that physiologic basis of RV_{DYS} in this subgroup differed from the remainder of our population and that heterogeneity in prior revascularization confounded our results. Moreover, our study population underwent imaging at a single center, and clinical status or prognostic outcomes in this cohort were not tested in relation to either RV function or NIF.

In conclusion, this study demonstrates that RV_{DYS} in patients with iMR is commonly associated with NIF on CMR and provides proof of concept concerning utility of multiplanar strain assessment for evaluation of RV_{DYS} and altered tissue substrate. Further studies are warranted to elucidate novel structural risk factors for iMR itself, whether NIF or strain based indices distinguish between iMR patients with persistent or reversible RV functional impairment, as well as prognostic implications of RV_{DYS} among patients with iMR.

Author Contributions

Conceptualization: Antonino Di Franco, Jonathan W. Weinsaft.

Formal analysis: Antonino Di Franco, Jiwon Kim, Aparna Srinivasan, Jonathan W. Weinsaft.

Funding acquisition: Jonathan W. Weinsaft.

Investigation: Antonino Di Franco, Jiwon Kim, Sara Rodriguez-Diego, Omar Khalique, Neil K. Mehta, Jonathan W. Weinsaft.

Methodology: Antonino Di Franco, Jonathan W. Weinsaft.

Project administration: Jonathan Y. Siden, Samantha R. Goldburg.

Resources: Jonathan Y. Siden, Mark B. Ratcliffe, Robert A. Levine.

Supervision: Antonino Di Franco, Jiwon Kim, Omar Khalique, Jonathan Y. Siden, Samantha R. Goldburg, Mark B. Ratcliffe, Robert A. Levine, Filippo Crea, Richard B. Devereux, Jonathan W. Weinsaft.

Validation: Antonino Di Franco.

Writing – original draft: Antonino Di Franco, Richard B. Devereux, Jonathan W. Weinsaft.

Writing – review & editing: Antonino Di Franco, Jiwon Kim, Sara Rodriguez-Diego, Omar Khalique, Jonathan Y. Siden, Samantha R. Goldburg, Neil K. Mehta, Aparna Srinivasan, Mark B. Ratcliffe, Robert A. Levine, Filippo Crea, Richard B. Devereux, Jonathan W. Weinsaft.

References

1. Polak JF, Holman BL, Wynne J, Colucci WS. Right ventricular ejection fraction: an indicator of increased mortality in patients with congestive heart failure associated with coronary artery disease. *J Am Coll Cardiol* 1983; 2:217–224. PMID: 6306086
2. Zornoff LAM, Skali H, Pfeffer MA, St John Sutton M, Rouleau JL, Lamas GA, et al. Right ventricular dysfunction and risk of heart failure and mortality after myocardial infarction. *J Am Coll Cardiol* 2002; 39:1450–1455. PMID: 11985906
3. Pennell DJ. Cardiovascular Magnetic Resonance. *Circulation* 2010; 121:692–705. https://doi.org/10.1161/CIRCULATIONAHA.108.811547 PMID: 20142462

4. Grothues F, Moon JC, Bellenger NG, Smith GS, Klein HU, Pennell DJ. Interstudy reproducibility of right ventricular volumes, function, and mass with cardiovascular magnetic resonance. *Am Heart J* 2004; 147:218–223. https://doi.org/10.1016/j.ahj.2003.10.005 PMID: 14760316
5. Kawut SM, Lima JAC, Barr RG, Chahal H, Jain A, Tandri H, et al. Sex and race differences in right ventricular structure and function: the multi-ethnic study of atherosclerosis-right ventricle study. *Circulation* 2011; 123:2542–2551. https://doi.org/10.1161/CIRCULATIONAHA.110.985515 PMID: 21646505
6. Freed BH, Gomberg-Maitland M, Chandra S, Mor-Avi V, Rich S, Archer SL, et al. Late gadolinium enhancement cardiovascular magnetic resonance predicts clinical worsening in patients with pulmonary hypertension. *J Cardiovasc Magn Reson* 2012; 14:11. https://doi.org/10.1186/1532-429X-14-11 PMID: 22296860
7. Gulati A, Jabbour A, Ismail TF, Guha K, Khwaja J, Raza S, et al. Association of fibrosis with mortality and sudden cardiac death in patients with nonischemic dilated cardiomyopathy. *JAMA* 2013; 309:896–908. https://doi.org/10.1001/jama.2013.1363 PMID: 23462786
8. Kjaergaard J, Petersen CL, Kjaer A, Schaadt BK, Oh JK, Hassager C. Evaluation of right ventricular volume and function by 2D and 3D echocardiography compared to MRI. *Eur J Echocardiogr* 2006; 7: 430–438. https://doi.org/10.1016/j.euje.2005.10.009 PMID: 16338173
9. Prakken NHJ, Teske AJ, Cramer MJ, Mosterd A, Bosker AC, Mali WP, et al. Head-to-head comparison between echocardiography and cardiac MRI in the evaluation of the athlete's heart. *Br J Sports Med* 2012; 46:348–354. https://doi.org/10.1136/bjsm.2010.077669 PMID: 21278426
10. Lai WW, Gauvreau K, Rivera ES, Saleeb S, Powell AJ, Geva T. Accuracy of guideline recommendations for two-dimensional quantification of the right ventricle by echocardiography. *Int J Cardiovasc Imaging* 2008; 24:691–698. https://doi.org/10.1007/s10554-008-9314-4 PMID: 18438737
11. Srinivasan A, Kim J, Khalique O, Geevarghese A, Rusli M, Shah T, et al. Echocardiographic linear fractional shortening for quantification of right ventricular systolic function-A cardiac magnetic resonance validation study. *Echocardiogr Mt Kisco N* 2017; 34:348–358.
12. Kim J, Srinivasan A, Seoane T, Di Franco A, Peskin CS, McQueen DM, et al. Echocardiographic Linear Dimensions for Assessment of Right Ventricular Chamber Volume as Demonstrated by Cardiac Magnetic Resonance. *J Am Soc Echocardiogr* 2016; 29:861–870. https://doi.org/10.1016/j.echo.2016.05.002 PMID: 27297619
13. Lindqvist P, Henein M, Kazzam E. Right ventricular outflow-tract fractional shortening: an applicable measure of right ventricular systolic function. *Eur J Echocardiogr* 2003; 4:29–35. PMID: 12565060
14. Palmieri V, Dahlöf B, DeQuattro V, Sharpe N, Bella JN, de Simone G, et al. Reliability of echocardiographic assessment of left ventricular structure and function: the PRESERVE study. Prospective Randomized Study Evaluating Regression of Ventricular Enlargement. *J Am Coll Cardiol* 1999; 34:1625–1632. PMID: 10551715
15. Kim J, Di Franco A, Seoane T, Srinivasan A, Kampaktsis PN, Geevarghese A, et al. Right Ventricular Dysfunction Impairs Effort Tolerance Independent of Left Ventricular Function Among Patients Undergoing Exercise Stress Myocardial Perfusion Imaging. *Circ Cardiovasc Imaging* 2016; 9. https://doi.org/10.1161/CIRCIMAGING.116.005115 PMID: 27903538
16. Rudski LG, Lai WW, Afilalo J, Hua L, Handschumacher MD, Chandrasekaran K, et al. Guidelines for the echocardiographic assessment of the right heart in adults: a report from the American Society of Echocardiography endorsed by the European Association of Echocardiography, a registered branch of the European Society of Cardiology, and the Canadian Society of Echocardiography. *J Am Soc Echocardiogr* 2010; 23:685–713; quiz 786–788. https://doi.org/10.1016/j.echo.2010.05.010 PMID: 20620859
17. Zoghbi WA, Enriquez-Sarano M, Foster E, Grayburn PA, Kraft CD, Levine RA, et al. Recommendations for evaluation of the severity of native valvular regurgitation with two-dimensional and Doppler echocardiography. *J Am Soc Echocardiogr* 2003; 16:777–802. https://doi.org/10.1016/S0894-7317(03)00335-3 PMID: 12835667
18. Volo SC, Kim J, Gurevich S, Petashnick M, Kampaktsis P, Feher A, et al. Effect of myocardial perfusion pattern on frequency and severity of mitral regurgitation in patients with known or suspected coronary artery disease. *Am J Cardiol* 2014; 114:355–361. https://doi.org/10.1016/j.amjcard.2014.05.008 PMID: 24948494
19. Jones EC, Devereux RB, Roman MJ, Liu JE, Fishman D, Lee ET, et al. Prevalence and correlates of mitral regurgitation in a population-based sample (the Strong Heart Study). *Am J Cardiol* 2001; 87:298–304. PMID: 11165964
20. Devereux RB, Alonso DR, Lutas EM, Gottlieb GJ, Campo E, Sachs I, et al. Echocardiographic assessment of left ventricular hypertrophy: comparison to necropsy findings. *Am J Cardiol* 1986; 57:450–458. PMID: 2936235

21. Devereux RB, Roman MJ, Palmieri V, Liu JE, Lee ET, Best LG, et al. Prognostic implications of ejection fraction from linear echocardiographic dimensions: the Strong Heart Study. *Am Heart J* 2003; 146:527–534. https://doi.org/10.1016/S0002-8703(03)00229-1 PMID: 12947374

22. Palmieri V, Roman MJ, Bella JN, Liu JE, Best LG, Lee ET, et al. Prognostic implications of relations of left ventricular systolic dysfunction with body composition and myocardial energy expenditure: the Strong Heart Study. *J Am Soc Echocardiogr* 2008; 21:66–71. https://doi.org/10.1016/j.echo.2007.05.008 PMID: 17628407

23. Devereux RB, Wachtell K, Gerdts E, Boman K, Nieminen MS, Papademetriou V, et al. Prognostic significance of left ventricular mass change during treatment of hypertension. *JAMA* 2004; 292:2350–2356. https://doi.org/10.1001/jama.292.19.2350 PMID: 15547162

24. Sievers B, Elliott MD, Hurwitz LM, Albert TSE, Klem I, Rehwald WG, et al. Rapid detection of myocardial infarction by subsecond, free-breathing delayed contrast-enhancement cardiovascular magnetic resonance. *Circulation* 2007; 115:236–244. https://doi.org/10.1161/CIRCULATIONAHA.106.635409 PMID: 17200443

25. Weinsaft JW, Kim J, Medicherla CB, Ma CL, Codella NCF, Kukar N, et al. Echocardiographic Algorithm for Post-Myocardial Infarction LV Thrombus: A Gatekeeper for Thrombus Evaluation by Delayed Enhancement CMR. *JACC Cardiovasc Imaging* 2016; 9:505–515. https://doi.org/10.1016/j.jcmg.2015.06.017 PMID: 26476503

26. Kim J, Medicherla CB, Ma CL, Feher A, Kukar N, Geevarghese A, et al. Association of Right Ventricular Pressure and Volume Overload with Non-Ischemic Septal Fibrosis on Cardiac Magnetic Resonance. *PloS One* 2016; 11:e0147349. https://doi.org/10.1371/journal.pone.0147349 PMID: 26799498

27. Swift AJ, Rajaram S, Capener D, Elliot C, Condliffe R, Wild JM, et al. LGE patterns in pulmonary hypertension do not impact overall mortality. *JACC Cardiovasc Imaging* 2014; 7:1209–1217. https://doi.org/10.1016/j.jcmg.2014.08.014 PMID: 25496540

28. Kim J, Kochav JD, Gurevich S, Afroz A, Petashnick M, Volo S, et al. Left ventricular geometric remodeling in relation to non-ischemic scar pattern on cardiac magnetic resonance imaging. *Int J Cardiovasc Imaging* 2014; 30:1559–1567. https://doi.org/10.1007/s10554-014-0487-8 PMID: 25008088

29. Kim J, Medicherla CB, Ma CL, Feher A, Kukar N, Geevarghese A, et al. Association of Right Ventricular Pressure and Volume Overload with Non-Ischemic Septal Fibrosis on Cardiac Magnetic Resonance. *PloS One* 2016; 11:e0147349. https://doi.org/10.1371/journal.pone.0147349 PMID: 26799498

30. Pavlicek M, Wahl A, Rutz T, de Marchi SF, Hille R, Wustmann K, et al. Right ventricular systolic function assessment: rank of echocardiographic methods vs. cardiac magnetic resonance imaging. *Eur J Echocardiogr* 2011; 12:871–880. https://doi.org/10.1093/ejechocard/jer138 PMID: 21900300

31. Alpendurada F, Guha K, Sharma R, Ismail TF, Clifford A, Banya W, et al. Right ventricular dysfunction is a predictor of non-response and clinical outcome following cardiac resynchronization therapy. *J Cardiovasc Magn Reson* 2011; 13:68. https://doi.org/10.1186/1532-429X-13-68 PMID: 22040270

32. Codella NCF, Cham MD, Wong R, Chu C, Min JK, Prince MR, et al. Rapid and accurate left ventricular chamber quantification using a novel CMR segmentation algorithm: a clinical validation study. *J Magn Reson Imaging* 2010; 31:845–853. https://doi.org/10.1002/jmri.22080 PMID: 20373428

33. Codella NCF, Weinsaft JW, Cham MD, Janik M, Prince MR, Wang Y. Left ventricle: automated segmentation by using myocardial effusion threshold reduction and intravoxel computation at MR imaging. *Radiology* 2008; 248:1004–1012. https://doi.org/10.1148/radiol.2482072016 PMID: 18710989

34. Grewal J, Majdalany D, Syed I, Pellikka P, Warnes CA. Three-dimensional echocardiographic assessment of right ventricular volume and function in adult patients with congenital heart disease: comparison with magnetic resonance imaging. *J Am Soc Echocardiogr* 2010; 23:127–133. https://doi.org/10.1016/j.echo.2009.11.002 PMID: 19962272

35. Leibundgut G, Rohner A, Grize L, Bernheim A, Kessel-Schaefer A, Bremerich J, et al. Dynamic assessment of right ventricular volumes and function by real-time three-dimensional echocardiography: a comparison study with magnetic resonance imaging in 100 adult patients. *J Am Soc Echocardiogr* 2010; 23:116–126. https://doi.org/10.1016/j.echo.2009.11.016 PMID: 20152692

36. Kim J, Cohen SB, Atalay MK, Maslow AD, Poppas A. Quantitative Assessment of Right Ventricular Volumes and Ejection Fraction in Patients with Left Ventricular Systolic Dysfunction by Real Time Three-Dimensional Echocardiography versus Cardiac Magnetic Resonance Imaging. *Echocardiogr Mt Kisco N* 2015; 32:805–812.

37. Lemarié J, Huttin O, Girerd N, Mandry D, Juillière Y, Moulin F, et al. Usefulness of Speckle-Tracking Imaging for Right Ventricular Assessment after Acute Myocardial Infarction: A Magnetic Resonance Imaging/Echocardiographic Comparison within the Relation between Aldosterone and Cardiac Remodeling after Myocardial Infarction Study. *J Am Soc Echocardiogr* 2015; 28:818–827.e4. https://doi.org/10.1016/j.echo.2015.02.019 PMID: 25840640

38. Park J-H, Negishi K, Kwon DH, Popovic ZB, Grimm RA, Marwick TH. Validation of global longitudinal strain and strain rate as reliable markers of right ventricular dysfunction: comparison with cardiac magnetic resonance and outcome. *J Cardiovasc Ultrasound* 2014; 22:113–120. https://doi.org/10.4250/jcu.2014.22.3.113 PMID: 25309687

39. Beeri R, Yosefy C, Guerrero JL, Abedat S, Handschumacher MD, Stroud RE, et al. Early repair of moderate ischemic mitral regurgitation reverses left ventricular remodeling: a functional and molecular study. *Circulation* 2007; 116:I288–293. https://doi.org/10.1161/CIRCULATIONAHA.106.681114 PMID: 17846319

40. Beeri R, Yosefy C, Guerrero JL, Nesta F, Abedat S, Chaput M, et al. Mitral regurgitation augments post-myocardial infarction remodeling failure of hypertrophic compensation. *J Am Coll Cardiol* 2008; 51:476–486. https://doi.org/10.1016/j.jacc.2007.07.093 PMID: 18222360

41. McKenzie JC, Kelley KB, Merisko-Liversidge EM, Kennedy J, Klein RM. Developmental pattern of ventricular atrial natriuretic peptide (ANP) expression in chronically hypoxic rats as an indicator of the hypertrophic process. *J Mol Cell Cardiol* 1994; 26:753–767. https://doi.org/10.1006/jmcc.1994.1090 PMID: 8089855

42. Taylor RJ, Umar F, Lin ELS, Ahmed A, Moody WE, Mazur W, et al. Mechanical effects of left ventricular midwall fibrosis in non-ischemic cardiomyopathy. *J Cardiovasc Magn Reson* 2016; 18:1. https://doi.org/10.1186/s12968-015-0221-2 PMID: 26732096

43. Muraru D, Onciul S, Peluso D, Soriani N, Cucchini U, Aruta P, et al. Sex- and Method-Specific Reference Values for Right Ventricular Strain by 2-Dimensional Speckle-Tracking Echocardiography. *Circ Cardiovasc Imaging* 2016; 9:e003866. https://doi.org/10.1161/CIRCIMAGING.115.003866 PMID: 26860970

44. Rösner A, Avenarius D, Malm S, Iqbal A, Schirmer H, Bijnens B, et al. Changes in Right Ventricular Shape and Deformation Following Coronary Artery Bypass Surgery-Insights from Echocardiography with Strain Rate and Magnetic Resonance Imaging. *Echocardiogr Mt Kisco N* 2015; 32:1809–1820.

45. Duncan AE, Sarwar S, Kateby Kashy B, Sonny A, Sale S, Alfirevic A, et al. Early Left and Right Ventricular Response to Aortic Valve Replacement. *Anesth Analg* 2017; 124:406–418. https://doi.org/10.1213/ANE.0000000000001108 PMID: 26702865